Pharmaceutical Sciences, 2022, 28(3), 405-413
doi:10.34172/PS.2021.64
https://ps.tbzmed.ac.ir/

Research Article

Expression, Purification and Characterization of Anti-FGF7 Domain Antibody Identified Using Phage Display Technique

Ali Akbar Alizadeh[1,2], Mona Roshani[1,3], Omid Jamshidi Kandjani[1], Milad Soltani-Saif[1,3], Siavoush Dastmalchi[1,3,4*]

[1]*Biotechnology Research Center, Tabriz University of Medical Sciences, Tabriz, Iran.*
[2]*Pharmaceutical Analysis Research Center, Tabriz University of Medical Sciences, Tabriz, Iran.*
[3]*School of Pharmacy, Tabriz University of Medical Sciences, Tabriz, Iran.*
[4]*Faculty of Pharmacy, Near East University, POBOX:99138, Nicosia, North Cyprus, Mersin 10, Turkey.*

Article Info

Article History:
Received: 5 September 2021
Accepted: 18 October 2021
ePublished: 27 October 2021

Keywords:
-Domain antibodies
-MD simulations
-Molecular docking
-FGF7
-Phage display

Abstract

Background: Fibroblast growth factors (FGFs) are involved in angiogenesis, wound healing and embryonic development. However, one of the causes of cancer cell growth in fibroblast-dependent cancers is FGF7 secreted by fibroblasts. Therefore, antibodies against FGF7 can be used for the treatment of these types of cancers.

Methods: In the previous studies, a phage displaying single domain antibody, D53, against human FGF7 has been identified using the phage display technique. In the present study, D53 was produced and purified in its isolated form. ELISA experiment was performed to evaluate the binding of D53 to FGF7. The mode of interaction of D53-FGF7 was explored using docking study and molecular dynamics (MD) simulations.

Results: The expression and purification processes were verified using western blotting and SDS-PAGE analyses. ELISA experiment showed that D53 is able to recognize and bind FGF7. Docking study and MD simulations indicated that compared to dummy V_H, D53 has more affinity towards FGF7.

Conclusion: The findings in the current study can be useful for the generation and the development of FGF7 inhibitors with a potential use in fibroblast-dependent cancers.

Introduction

Fibroblast growth factors (FGFs) are a family of single-chain polypeptides that control a wide range of cellular processes including proliferation, angiogenesis, cell survival, differentiation and migration.[1] Abnormal increases in the FGF gene expression lead to various diseases in humans.[2] FGFs were first found in 1973 in pituitary extract[3] with a molecular weight of 17-29 kDa and their core contains 120-130 amino acids.[4] So far, 23 members of the FGF family have been identified, which are classified into three categories based on the mechanism: endocrine, paracrine, and intracellular.[5] FGFs induce proliferation, angiogenesis, cell survival, differentiation and migration of cancer cells.[6] They produce signals by binding to four different receptors, which include FGFR 1-4 and are encoded by four distinct genes.[7] FGF receptors contain an extracellular ligand domain composed of three immunoglobulin-like domains (D1, D2, D3), a transmembrane helix domain, and an intracellular domain with tyrosine kinase activity.[8,9] These receptors are dimerized upon ligand (FGF) binding followed by the intracellular domain phosphorylatation which leads to the activation of different signal pathways.[10,11] Each receptor can be activated by several types of FGF, and each FGF can activate more than one type of receptor. However, Fibroblast growth factor 7 (FGF7) binds very specifically to FGFR2IIIb (also called KGFR) receptor for exerting its biological role.[12,13] FGF7 is a polypeptide with a molecular weight of 28 kDa.[14] This growth factor is a part of a 23-membered FGF family and is the product of KGF gene, which contains 3 exons and 2 introns.[15,16] FGF7 was first identified in human fetal pulmonary fibroblasts and purified as a soluble factor secreted by stromal fibroblasts. This protein is expressed in lungs, prostate, mammary glands, gastrointestinal tract, bladder and skin[17,18] and is a suitable mitogen for epithelial cells for differentiation, migration and angiogenesis.[12] In physiological levels, FGF7 induces cell growth and differentiation during the embryonic period, puberty and adulthood, and promotes homeostasis.[19] However, in pathological levels FGF7 has been implicated in cancers with fibroblastic origin called Carcinoma Associated Fibroblasts (CAFs). Investigation using lingual cancer cells showed that FGF7 secreted by

*Corresponding Author: Siavoush Dastmalchi, E-mail: dastmalchi.s@tbzmed.ac.ir

CAFs is one of the main factors in the growth of CAFs cancer cells.[19] Phage display is a conventional technique that can be used to identify new ligands against receptors and enzymes for drug design and identification of polyclonal or monoclonal antibodies as the therapeutic agents,[20] In phage display, various antibody formats including single-chain fragment variable antibody (scFv), domain antibody (dAb) and Fab antibody are displayed on phage particles which can be subsequently used to isolate antibodies capable of binding against target of interest.[21] These formats of antibodies are more widely used in research and industry, and their properties are optimized for binding affinity, stability, pharmacokinetic properties, and expression levels.[22] Domain antibodies are small in size, cost-effective to produce, and can be easily modified genetically. Moreover, they are more prone for crossing the blood-brain barrier and penetrating tumors.[23] The current study aimed to characterize the binding ability of previously identified single domain antibody (sdAb) called D53 against FGF7 with a potential use for the treatment of cancers where CAFs are involved. For this, the coding gene corresponding to D53 was inserted into pGEX-6P-1 bacterial expression system at the downstream of glutathione S-transferase (GST) coding gene. The genetically engineered vector enabled the expression of dAb attached to GST which facilitated the purification process using glutathione sepharose affinity column. ELISA experiment was used to evaluate the binding ability of D53 to FGF7. The mode of interaction of D53 with FGF7 was also explored using *in silico* methods where three-dimensional models for D53 and FGF7 were constructed and used in docking study. The obtained complex of D53-FGF7 through docking calculation was subjected to MD simulations where the structural stability of the complex and the binding ability of D53 to FGF7 were explored and compared to that of a dummy V_H.

Materials and Method

Materials

PCR master was purchased from Bioron, Germany. Restriction enzymes and T4 ligase were from Fermentas, USA. NaCl and 3,3′,5,5′-Tetramethylbenzidine (TMB) were obtained from Sigma Aldrich (USA). Tryptone, yeast extract, isopropyl-b-D-thio galactopyranoside (IPTG), Triton X-100, phenylmethylsulfonyl fluoride (PMSF) and N,N,N',N'-tetramethylethylenediamine (TEMED) were purchased from AppliChem (Darmstadt, Germany). Glutathione Sepharose 4B was prepared from GE Healthcare Life Sciences (Sweden). Agarose was from Invitrogen Ltd (Paisley, UK). Methanol, β-mercaptoethanol and triethylamine (TEA) were from Merck, Germany. Primers used in this work were ordered from Pishgam Biotech (Tehran, Iran). Acrylamide and N,N'-methylene-bis-acrylamide were purchased from CinnaGen (Tehran, Iran). All chemicals and reagents were of molecular biology grade. Milli-Q water (Millipore Corporation, Bradford, MA, USA) was used for the preparation of all solutions. The pGEX-2T (Catalog No: 45-002-278, GE healthcare) was a gift from Prof. Joel Mackay at Sydney University, Australia.

Gene cloning

In our previous study using phage display technique, phage presenting D53 domain antibody was identified as a FGF7 binder, however, the identification of this antibody was not reported there.[24] Investigating the DNA sequence for the identified dAb, i.e., D53, showed the presence of an amber stop codon in the coding sequence, which was located in the CDR2 region of D53 coding gene. In the present study, the site directed point mutation method was used to convert the first codon position of amber (TAG) stop codon to C, so that it can code for the desired residue (glutamine) in D53 protein. For this, overlapping primers were designed using PrimerX site (https://www.bioinformatics.org/primerx). The sequence of primers designed for this purpose and other primers used in this study are as follows: Forward (F1) 5'-CAGGGATCCATG GCCCAGGTGCAG-3' and Reverse (R1) 5' –TTCGAATTCTCAGCTCGAGAC-GGTGACCAG-3' and Overlapping Primers Forward (F2) 5'- GATTTAGCGTTAGCCATGAGAATATGACCTGGG -3 and Reverse (R2) 5'- GACCCAGGTCATATTCTCAT-GGCTAACGCTAAA – 3'. The gene fragment was located inside the phage vector pR2. Therefore, in the first step, F1 and R2 primers were used where pR2 vector was used as the template DNA. In the second step, primers F2 and R1 were employed using the same DNA template. Two PCR products from the first and second steps were used as the template DNA to carry out the third PCR reaction using F1 and R1 primers. The product obtained from the third step, which was a complete gene fragment, was used for cloning into pGEX-6P-1 vector. PCR reaction followed by the gene sequencing was utilized to confirm successful point mutation and cloning. For this, the recombinant plasmid pGEX-6P-1 harboring D53 coding gene was transformed into *E.coli BL21 (DE3)* cells and plated on LB medium supplemented with amplicillin (100 m g/mL). Individual colonies were used to inoculate 10 mL LB-ampicillin medium and grow overnight at 37 °C while shaking. The vector was extracted and PCR reaction using F1 and R1 primers were conducted and agarose gel electrophoresis was used for analysis. Final confirmation was carried out by gene sequencing. As a control, the coding gene of a dummy V_H was amplified using F1 and R1 primers and after digestion was cloned into pGEX-6P-1 vector.

Expression and purification of D53

The recombinant plasmid was transformed into *E.coli Origami* expression strain for producing D53 recombinant protein attached to GST protein. The expression and purification of interest protein was performed as described in our previous work.[25] Briefly, 10 mL of LB-ampicillin medium was inoculated using a single colony and incubated at 37 °C for 16 h while shaking at 180 rpm. Next day, the grown culture was diluted 1:50 into a 200 mL

2TY medium and cultivated in a shaker-incubator at 180 rpm and 37 °C until OD_{600} 0.9. After reaching the desired OD, to induce protein production, IPTG with a final concentration of 0.4 mM was added to the culture medium and incubation was continued at 20 °C for additional 3 h while shaking with 180 rpm. To examine the expression of protein, samples were taken at different time intervals (before adding IPTG, 1 h and 2 h after adding IPTG). After 3 h, the cells were harvested by centrifugation for 10 min at 4 °C at 5000 rpm and suspended in lysis buffer containing Tris 50 mM pH 8, NaCl 150 mM, Triton 1%, lysozyme 0.1 mg/mL, DNAse 10 µg/mL, β-mercaptoethanol 0.1%, PMSF 1.4 mM. Using three cycles of freeze-thaw followed by five times sonication on ice at 60 % pulse for 30 s with 30 s pauses between pulses, the cells were disrupted and the soluble fractions containing the interest dAbs attached to GST were separated from the bacteria debris. The soluble fractions were subjected to glutathione sepharose affinity column and after washing by five column volumes wash buffer (Tris 50 mM, NaCl 150 mM, β-Mercaptoethanol 0.1%), the dAb-GST fusion proteins were released from the column using elution buffer containing glutathione 10 mM and Tris 50 mM. SDS-PAGE analysis was carried out to monitor the protein expression and purification steps.

Western blotting

Protein samples were resolved on SDS-PAGE and then the protein bands were transferred on a PVDF membrane at 250 mA current for 30 min, at 4 °C. The membrane was blocked overnight using 5 % skim milk prepared in TBS buffer (Tris 20 mM, NaCl 100 mM) and after washing by TBS it was incubated 2 h at room temperature with HRP-conjugated anti GST antibody (Santa Cruz Biotechnology, USA) diluted 1:200 in 3 % skim milk. The membrane was washed five times by TBST buffer (TBS with 0.1 % tween 20) and using the ECL solution and in the presence of H_2O_2 (oxidizing agent), the produced signals were recorded on negative film.

ELISA experiment

ELISA experiment was performed to evaluate the binding ability of the produced D53 to FGF7. For this purpose, 100 mL D53-GST with 85 mg/mL concentration was added to each well of a 96-well plate and the plate was incubated overnight at 4 °C in a humidified atmosphere. The next day, the contents of the wells were discarded and washed three times with 200 µL of TBS buffer. From 2 % solution of BSA, 200 µL was added to each well and incubated for 2 h at room temperature. Wells were washed twice using TBS and then various concentrations of FGF7 diluted in TBS (19 µM, 6.3 µM, 2.1 µM, 0.7 µM and 0.23 µM, 0.7 µM) were added to the wells. FGF7 was produced according to the protocol described previously [24]. After 2 h incubation, the wells were washed three times using TBST and mouse anti-FGF7 antibody was added to the wells and the plate was incubated for further 2 h at room temperature. Goat HRP-conjugated anti-mouse IgG diluted with 2% BSA solution was added to each well and incubated for 1 h at room temperature. The wells were washed four times using TBST and TMB solution was added to the well. The reaction was terminated after 15 min using 1 M H_2SO_4 and using ELISA plate reader the absorbance of wells were read at 450 nm and subtracted from their absorbance at 650 to eliminate the background effect. The obtained data were fit into one-site specific binding algorithm using prism program and the Kd binding of D53 to FGF7 was calculated. Dummy VH was used as the negative control.

Model building and MD simulations

Three dimensional models for D53, dummy V_H and FGF7 were constructed using I-TASSER program where 10 best templates selected from the LOMETS threading programs based on Z-score were used for the modeling.[26] The amino acid sequence of human FGF7 without signal peptide was retrieved from UniProtKB database (https://www.uniprot.org/uniprot/P21781) and used for model building based on rat FGF7 crystal structure (PDB ID: 1QQK). Permissible torsion angles were checked by Ramachandran diagram on PROCHECK site. Verify-3D software was used to determine the compatibility of the amino acid sequence with the assumed three-dimensional structures.[27,28] After model verification, the generated models of D53 and dummy V_H were docked into FGF7 model structure using Z-DOCK software and the possible protein-protein interactions were predicted at the PIC website.[29] The stabilities of generated D53-FGF7 complex and its binding energy were explored using MD simulations performed using the Assisted Model Building with Energy Refinement (AMBER) suite of programs (version 14) operating on a Linux-based (Centus 6.8) GPU work station. The corresponding AMBER input files for the complex were generated by leap module using Amber99 force-field. After neutralizing the system by addition of Cl^- ions, the system was solvated in a rectangular box with buffering distances of 12 Å in all directions using TIP3P water molecules and subjected into a short energy minimization process carried out by Sander module (500 steps of steepest descent followed by 500 steps of conjugate gradient). Subsequently, the system was equilibrated using a 50 ps heating step (increasing the temperature from 0 to 27 °C), a 50-ps density equilibration, followed by constant pressure equilibration for 500 ps at 27 °C with a time step of 2 fs. , Bond lengths involving hydrogen atoms were constrained by applying SHAKE algorithm. Long-range electrostatic interactions were calculated using particle mesh Ewald (PME) method in which the system was simulated for 50 ns. Every 10 ps, the coordinates were written out to obtain the trajectories of the simulation which were used subsequently to assess the stability parameters of complex.

Results and Discussion

Domain antibodies are a class of therapeutic proteins derived from the heavy chain variable domain of antibodies and, like a complete antibody, can bind selectively to

a specific antigen. Single-domain antibodies were first detected in 1993 by Harmer in the Camelidae family. They are derived from VHH of camel and cartilaginous fish called V-NAR, and the findings showed that the role of heavy chain variable region of an antibody in identifying target an antigen is greater than that of its light chain counterpart. This led to the design of single-domain antibodies devoid of light chain called domain antibodies.[30] Domain antibodies with a molecular weight of 11-15 kDa are the smallest pieces of protein that bind to antigen. This antibody format has higher solubility and unlike conventional antibodies can retain their function after incubation at high temperatures and denaturant condition which is attributed to their effective structural flexibility.[31] Studies have shown that domain antibodies are stable over a wide range of temperature which provides advantages over complete antibodies.[32] In terms of clinical applications, the smaller size of domain antibodies compared to whole antibodies (15 kDa vs. 150 kDa) enables their faster penetration into tissues and solid tumors which makes them suitable drug delivery vehicles for rapid transmitting of therapeutic agents such as radioactive materials to the target cells.[33] All these and many more desired features have led to their use in the diagnosis and treatment of cancer. Phage display technique is a method of identifying and isolating specific peptides and antibodies against target antigens and molecules. In this method, the gene encoding a diverse set of antibodies or peptides is inserted into the phage genome, eventually creating a library in which each phage represents a specific antibody or peptide. The sequence encoding an antibody or peptide is usually inserted into the N-terminal portion of the gene encoding one of the phage coat proteins so that the phage can produce the desired antibody or peptide bound to the coat protein at its surface. Through a process called biopanning, specific phage displayed antibodies can be isolated against any molecule of interest. In the previous study, some phage displaying domain antibodies were identified as FGF7 binders among them was phage displaying D53 domain antibody.[24] At the same concentration phage displaying D53 domain antibody showed significantly higher affinity towards FGF7 compared to a phage displaying dummy V_H domain antibody (p value < 0.01 in t-Test: Paired Two Sample for Means) (Figure 1). The current study was intended to produce D53 in its isolated form and evaluate its FGF7 binding properties. The binding capability of D53 to FGF7 was also investigated using *in silico* approaches such as molecular docking and MD simulations and the results were compared to that of the dummy V_H domain antibody.

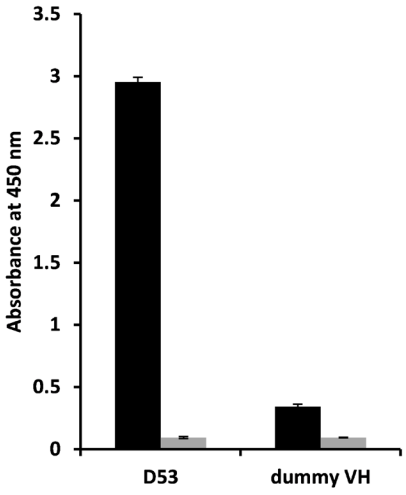

Figure 1. Evaluation of FGF7 binding capability of phage particles displaying D53 and a dummy VH single-domain antibody using ELISA experiment. Phage displaying D53 was identified using phage display technology conducted previously [24] where FGF7 protein coated in an ELISA plate was treated by phage displaying domain antibodies followed by detection of bound particles using horseradish peroxidase (HRP)–anti-M13 antibody. Phage displaying a dummy V_H was used for comparison. The black and gray columns are the results for wells coated and uncoated with FGF7.

Cloning of DNA sequences of D53 into pGEX-6P-1

Cloning process was performed as described previously.[34] Briefly, D53 coding gene located in phage pR2 genome were amplified and inserted into pGEX-6P-1 vector. However, DNA sequencing revealed the presence of an amber stop codon in the CDR2 region of D53, which is a problem frequently observed in phage display libraries.[34,35] The problem was resolved using site directed point mutation using overlap extension PCR mutagenesis technique to convert TAG amber stop codon into CAG to

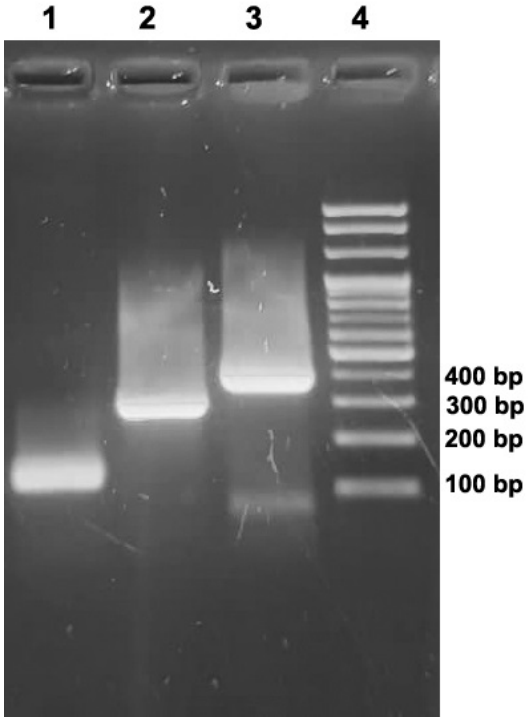

Figure 2. PCR reactions for site directed mutagenesis. Lane 1 is the PCR product using F1 and R2 primers. Lane 2 is related to the product of PCR reaction using F2 and R1 primers and lane 3 stands for the complete DNA sequence of D53 obtained using F1 and R1 priemrs where the products of lane 1 and 2 were used as the templates.

```
CLUSTAL O(1.2.4) multiple sequence alignment

                                           CDR1                    CDR2
D53          QVQLLESGGGLVQPGGSLRLSCAASGFSVSHENMTWVRQAPGKGLEWVSSITKAGGSTYY 60
dummy_VH     QVQLLESGGGLVQPGGSLRLSCAASGFTFSSYAMSWVRQAPGKGLEWVSAISGSGGSTYY 60
             ***************************:.*   *:**************:*: :******

                                                      CDR3
D53          ADSVKGRFTISRDNSKNTLYLQMNSLRAEDTAVYYCARRQRRWPKQMQYWGHGTLVTVSS 120
dummy_VH     ADSVKGRFTISRDNSKNTLYLQMNSLRAEDTAVYYCAKSYG----AFDYWGQGTLVTVS- 115
             *************************************.         ..***.*******
```

Figure 3. Amino acid sequences of D53 and dummy V_H. The CDRs have been highlighted on the sequences.

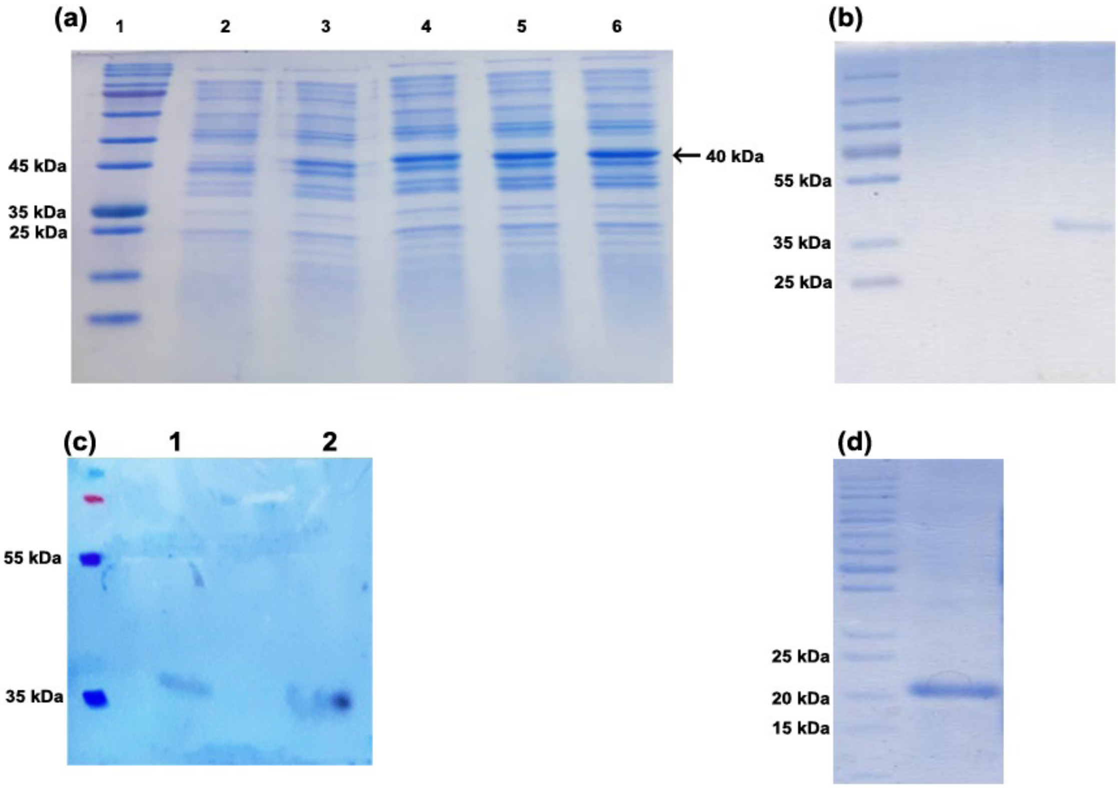

Figure 4. SDS-PAGE and western blotting analyses of D53 and FGF7. In panel (a), lane 1 is protein marker and lanes 2 through 6 are samples taken from expression culture of D53-GST before and 1, 2, 3 and 4 h after addition induction by IPTG. The appearance of a 40 kDa protein band after 3 and 4 hours induction indicates the increased protein expression during the time. Panel (b) shows the successful purification of D53 attached to GST with molecular weight of 40 kDa. Panel (c) is the western blot analysis of purified D53-GST protein (lane 1) and soluble fraction of sample taken 4 h after IPTG addition (lane 2). Panel (d) represents the production of FGF7 as a pure 6*His tagged 20 kDa protein. The process, expression vector and platform were the same as the protocol represented in Ref. 24.

code for amino acid glutamine. As outlined in Materials and methods section, during first two steps of mutation process, two separate DNA segments with the sizes of 123 bp and 297 bp were produced, which then were used together as the templates in the third step of PCR reaction to obtain a 384 bp DNA fragment encoding D53 (Figure 2).

The amplified DNA fragment was cloned into pGEX-6P-1 vector at the downstream of GST coding gene. The generated construct enabled the expression of D53 fused to GST which facilitated their purification process using glutathione sepharose affinity column. Cloning process was confirmed using PCR reactions and DNA sequencing, and pairwise sequence alignment between D53 coding sequences before and after site directed mutagenesis showed that the amber stop codon has been successfully converted to the glutamine codon. The coding gene of a V_H dummy was also amplified and cloned into pGEX-6P-1 vector to use as the negative control in all experiments. Using pairwise alignment, as shown in Figure 3, the amino acid sequences of D53 and dummy V_H were compared and the differences in CDR segments were highlighted.

Expression of domain antibodies

In the present study, D53 was produced attached to GST for

facilitating its purification using affinity chromatography on glutathione sepharose affinity column where GST serves as affinity ligand. The constructed pGEX-6P-1 vector harboring D53 coding gene was transformed into the prokaryotic system of *E. coli Origami (DE3)*. IPTG was used to stimulate the expression of engineered protein. Samples prepared during the protein expression process (before and at different time intervals after adding IPTG) were evaluated by SDS-PAGE method. The best results were observed when the induction was continued for 3 h and further induction time resulted in the formation insoluble GST-D53 fusion protein. As seen in Figure 4a, during 3 h expression as culture time increases the expression of 40 kDa D53 protein fused to GST increases as well (Figure 4a). SDS-PAGE analysis on affinity purified sample indicated the presence of a single band 40 kDa attributed to D53-GST fusion protein (Figure 4b). Using Bradford assay the concentrations of purified D53-GST fusion protein was measured to be 85 µg/mL. Western blot technique was used to confirm the protein expression in *E. coli Origami (DE3)* expression system and the success of purification of the expressed protein. Here, HRP-conjugated anti-GST antibody was used to confirm the production of the fusion protein. As shown in Figure 4c, the results of Western blot experiment confirm the successful expression and purification of D53-GST fusion protein (Figure 4c).

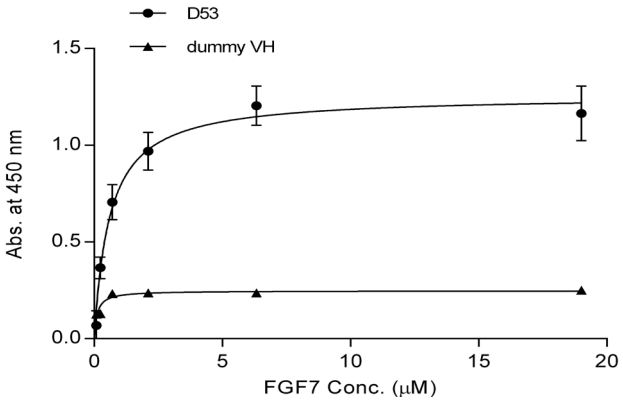

Figure 5. Evaluation of FGF7 binding capability of D53 using ELISA experiment. Various concentrations of FGF7 were added to the D53 coated wells. Subsequently, mouse anti-6×His and goat anti-mouse HRP-conjugated antibodies were used for protein detection. The calculated K_d binding of D53 to FGF7 was 0.6 ± 0.1 mM. A dummy VH domain antibody was used as the control which showed no affinity towards FGF7. All data are the means of triplicate ± S.D.Prism program (version 6.01, Graphpad Software Inc.) was used for data analysis.

ELISA experiment

ELISA experiment was performed to assess the ability of D53 antibody domain to bind FGF7 and compare it to that of dummy V_H domain antibody (negative control). For this purpose, the produced FGF7 (Figure 4d) was serially diluted and added to the ELISA plate wells previously coated with D53-GST fusion protein. Then, anti-6×His mouse antibody followed by HRP conjugated goat anti mouse antibody was used to evaluate the binding of D53 to FGF7. The absorbances recorded at 450 nm were fit into one-site specific binding model implemented in Prism program and the calculated K_d for binding of D53 towards FGF7 was 0.60 ± 0.10 m M. The dummy V_H domain antibody (negative control) used as the control showed no affinity towards FGF7 (Figure 5).

Molecular modeling of anti-FGF7 dAbs

To investigate the mode of interactions, three-dimensional structures of dummy V_H (negative control), D53 and FGF7 were constructed using I-TASSER program.[36] According to the Ramachandran plots generated by PROCHECK and MolProbity programs, 100% of the amino acids were in the allowed regions in terms of main chain Phi and Psi torsion angles. Results from Verify-3D assessment showed that the 3D-1D scores for 98.33, 98.26 and 83.44 % (more than

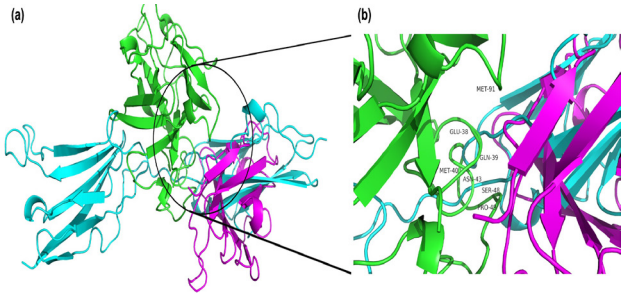

Figure 6. Cartoon representations of FGF7 (green) interactions with FGFR2 (cyan) and D53 (purple). Panel (a) represents the overlap between the FGFR2 and D53 binding sites on FGF7. In panel (b) the residues of FGF7 interacting with both FGFR2 and D53 have been highlighted in stick representation. PyMol (version 1.5.0.3) was used for production of images.

Table 1. The results of protein interaction analyses on D53-FGF7 and FGFR2-FGF7 complexes using PIC web server. The interactions involved FGF7 residues recognized by both D53 and FGFR2 were shown.

Interaction type	FGF7 residue number	D53 residue number	FGFR2 residue number
Hydrophobic contacts	Met40	Trp110	Ala168
	Pro49	Trp110, Leu45, Tyr95	Ala168, Leu246, Val248, Val249
	Met91	Leu5	Leu166
Hydrogen bonds	Glu38	Gln39	His167, Ala168, Val169
	Gln39	Tyr95, Gly111, His112	Leu166, His167, Ala168
	Asn43	Gln39, Tyr95	Val169, Asp247
	Ser48	Gln39	Val248, Asp247, Val248, Val249
	Pro49	Trp110	Asp247

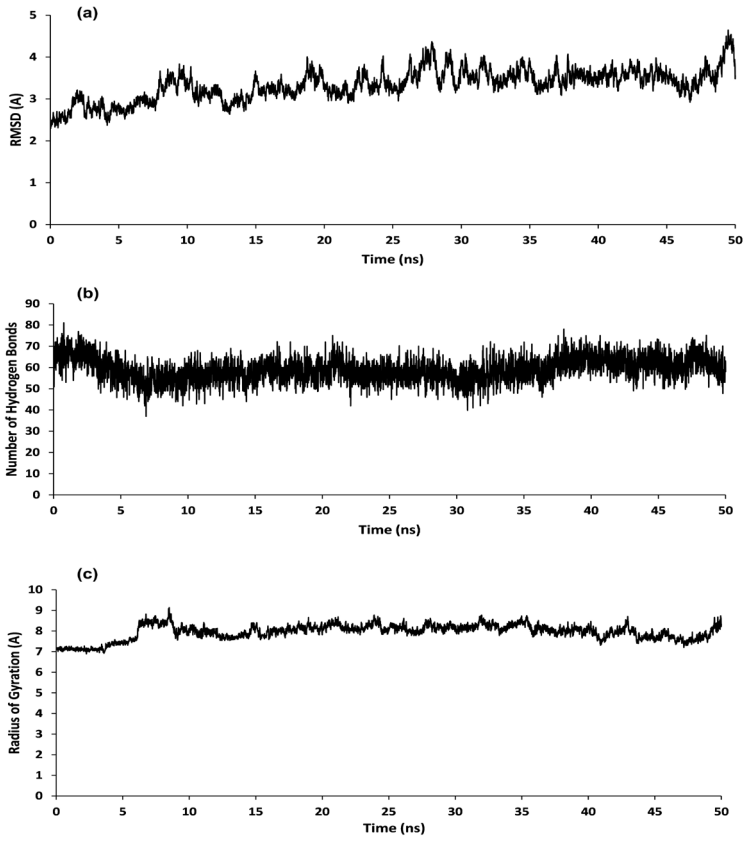

Figure 7. Panel (a) shows the RMSD alterations for D53-FGF7 during 50 ns MD simulations. Panel (b) corresponds to the variations in the number of hydrogen bonds during 50 ns simulation indicating low structural fluctuations. Panel (c) shows the alterations in radius of gyration for D53-FGF7 during 50 ns MD simulations indicating the structural stability of built model.

80%) of residue positions, respectively in D53, dummy V_H and FGF7 model structures were above the threshold value of 0.2 indicating the compatibility of the sequences with their assumed three-dimensional structures in the developed models. After evaluating the models, the modes of interactions of D53 and dummy V_H structural models with FGF7 model structure were predicted using molecular docking studies performed by Z-dock algorithm. The docking scores for D53-FGF7 and dummy V_H-FGF7 complexes were 1314 and 937, respectively, indicating more preferred affinity of D53 to FGF7 compared to that of control dummy V_H dAb. In order to investigate the details of interactions between D53 and FGF7, the obtained complexes from the docking calculations were evaluated by PIC (Protein interactions calculator) method from its webserver. For the purpose of comparison, a 3D model for FGFR2-FGF7 was constructed by superpositioning the built human FGF7 model on FGF10 structure in the experimentally solved FGF10-FGFR2 complex (PDB ID 1NUN). Then, both D53-FGF7 and FGFR2-FGF7 model complex structures were analyzed by PIC method and the residues of FGF7 chain recognizable by both D53 and FGFR2 were extracted (Table 1). The results illustrated in Figure 6 compares the modes of interactions of D53 and FGFR2 with FGF7 in D53-FGF7 and FGFR2-FGF7 model complexes. As shown in Table 1 and Figure 6, it seems that D53 could bind to those residues of FGF7 which is essential for the binding to its receptor FGFR2. Close inspection of the results revealed that CDR3 of D53 is its most essential segment to establish interactions with FGF7 as residues Tyr95, Trp110, Gly111 and His112 from CDR3 region of D53 are frequently taking part in the D53-FGF7 complex formation. The same analysis using PIC method was carried out on the dummy V_H-FGF7 complex and the results indicated the lack of common interactions between dummy V_H-FGF7 and FGFR2-FGF7 complexes. These findings may support that D53 dAb can be considered as an effective and specific FGF7 binder capable of interfering with FGF7-FGFR2 interaction in fibroblast-dependent cancers.

MD simulation study on dAbs-FGF7 complexes

In order to investigate the structural stability of modeled D53-FGF7 complex and also to calculate its binding energy, MD simulations were performed using Amber-ff99SB force fields available in AMBER 14. The modeled D53-FGF7 complex structure obtained by docking calculation was used for generating input files required for MD studies. The plots of root-mean-square deviation (RMSD), radius of gyration and number of hydrogen bonds during 50 ns simulations for the generated complex of D53-FGF7 are shown in Figure 7. The mean RMSD, number of hydrogen bonds and radius of gyration during 50 ns simulations were 3.34 ± 0.38, 59± 5.00 and 7.90± 0.37, respectively,

indicating the structural stability of the generated complex. Employing MM-GBSA algorithm implemented in Amber package, the ΔG° of binding energy for D53-FGF7 interaction calculated based on 50 ns simulation was -41.81 kcal.mol^{-1}, which was greatly smaller than that of dummy V_H-FGF7 complex (-18.57 kcal.mol^{-1}) further confirming the specific recognition of FGF7 by D53. These findings, in line with other results presented in this study, indicate that D53 can be considered as an effective and specific FGF7 binder which may interfere with FGF7-FGFR2 interaction.

FGF7 effectively contributes to CAFs vasculation and angiogenesis in tumors.[37] Therefore, many efforts have been devoted to inhibit FGF7-FGFR2 signaling pathways. This inhibition is mostly focused on identification of FGFR2 antogonists.[38,39] Identification of FGF binders can also be considered as a suitable strategy for disrupting FGF-FGFR2 signaling pathway. Although no drug has been approved from this class of inhibitors, however, some FGF binders such as FP-1039 (GSK3052230, GlaxoSmithKline) are in clinical trials for the purpose of cancer treatment. All these indicate that the identified anti-FGF7 antibody in the current study may present clinical significance in CAFs related cancers.

Conclusion

Previously, we isolated a phage displaying single domain antibody D53 against human FGF7 identified using phage display technique. In the present study, D53 was produced and purified in its isolated form. The expression and purification processes were verified using western blotting and SDS-PAGE analyses. ELISA experiment showed that D53 is able to specifically bind FGF7. The mode of interaction of D53 with FGF7 was assessed using docking study and molecular dynamics simulation. The results indicated that compared to a dummy V_H dAb, D53 has more affinity towards FGF7. The findings in the current study can be useful for the generation and the development of FGF7 inhibitors with the potential use in fibroblast-dependent cancers.

Author Contributions

AAA: Formal analysis, Writing - Original Draft, Project administration, Methodology and Revising manuscript; MR: Investigation and Methodology; OJ: Writing - Original Draft and Methodology; MSS: Investigation and Methodology; SD: Conceptualization, Validation, Supervision, Funding acquisition.

Acknowledgements

This work was supported by Research Office of Tabriz University of Medical Sciences [grant number 58596]. The authors would like to thank Biotechnology Research Center of for providing financial and facility supports.

Conflict of Interest

The authors report no conflicts of interest.

References

1. Li X, Wang C, Xiao J, McKeehan WL, Wang F. Fibroblast growth factors, old kids on the new block. Semin Cell Dev Biol. 2016;53:155-67. doi:10.1016/j.semcdb.2015.12.014
2. Burgess WH, Maciag T. The heparin-binding (fibroblast) growth factor family of proteins. Annu Rev Biochem. 1989;58:575-606. doi:10.1146/annurev.bi.58.070189.003043
3. Yun YR, Won JE, Jeon E, Lee S, Kang W, Jo H, et al. Fibroblast growth factors: Biology, function, and application for tissue regeneration. J Tissue Eng. 2010;2010:218142. doi:10.4061/2010/218142
4. Olsen SK, Garbi M, Zampieri N, Eliseenkova AV, Ornitz DM, Goldfarb M, et al. Fibroblast growth factor (fgf) homologous factors share structural but not functional homology with fgfs. J Biol Chem. 2003;278(36):34226-36. doi:10.1074/jbc.M303183200
5. Itoh N, Nakayama Y, Konishi M. Roles of fgfs as paracrine or endocrine signals in liver development, health, and disease. Front. Cell Dev. Biol. 2016;4:30. doi:10.3389/fcell.2016.00030
6. Hui Q, Jin Z, Li X, Liu C, Wang X. Fgf family: From drug development to clinical application. Int J Mol Sci. 2018;19(7):1875. doi:10.3390/ijms19071875
7. Porta R, Borea R, Coelho A, Khan S, Araújo A, Reclusa P, et al. Fgfr a promising druggable target in cancer: Molecular biology and new drugs. Crit Rev Oncol Hematol. 2017;113:256-67. doi:10.1016/j.critrevonc.2017.02.018
8. Brady N, Chuntova P, Bade LK, Schwertfeger KL. The fgf/fgfr axis as a therapeutic target in breast cancer. Expert Rev Endocrinol Metab. 2013;8(4):391-402. doi :10.1586/17446651.2013.811910
9. Powers CJ, McLeskey SW, Wellstein A. Fibroblast growth factors, their receptors and signaling. Endocr Relat Cancer. 2000;7(3):165-97. doi:10.1677/erc.0.0070165
10. Dai S, Zhou Z, Chen Z, Xu G, Chen Y. Fibroblast growth factor receptors (fgfrs): Structures and small molecule inhibitors. Cells. 2019;8(6):614. doi:10.3390/cells8060614
11. Itoh N, Ornitz DM. Fibroblast growth factors: From molecular evolution to roles in development, metabolism and disease. J Biochem. 2011;149(2):121-30. doi:10.1093/jb/mvq121
12. Sher I, Yeh BK, Mohammadi M, Adir N, Ron D. Structure-based mutational analyses in fgf7 identify new residues involved in specific interaction with fgfr2iiib. FEBS Lett. 2003;552(2-3):150-4. doi:10.1016/s0014-5793(03)00909-8
13. Zhang X, Ibrahimi OA, Olsen SK, Umemori H, Mohammadi M, Ornitz DM. Receptor specificity of the fibroblast growth factor family. The complete mammalian fgf family. J Biol Chem 2006;281(23):15694-700. doi:10.1074/jbc.M601252200
14. Aaronson SA, Bottaro DP, Miki T, Ron D, Finch

PW, Fleming TP, et al. Keratinocyte growth factor. A fibroblast growth factor family member with unusual target cell specificity. Ann N Y Acad Sci. 1991;638:62-77. doi:10.1111/j.1749-6632.1991.tb49018.x
15. Babina IS, Turner NC. Advances and challenges in targeting fgfr signalling in cancer. Nat Rev Cancer, 2017;17(5):318-32. doi:10.1038/nrc.2017.8
16. Turner N, Grose R. Fibroblast growth factor signalling: From development to cancer. Nat Rev Cancer. 2010;10(2):116-29. doi:10.1038/nrc2780
17. Rubin JS, Bottaro DP, Chedid M, Miki T, Ron D, Cheon G, et al. Keratinocyte growth factor. Cell Biol Int. 1995;19(5):399-411. doi:10.1006/cbir.1995.1085
18. Yen TT, Thao DT, Thuoc TL. An overview on keratinocyte growth factor: From the molecular properties to clinical applications. Protein Pept. Lett. 2014;21(3):306-17. doi:10.2174/0929866511320666011 5
19. Finch PW, Rubin JS. Keratinocyte growth factor/ fibroblast growth factor 7, a homeostatic factor with therapeutic potential for epithelial protection and repair. Adv Cancer Res. 2004;91:69-136. doi:10.1016/ s0065-230x(04)91003-2
20. McCafferty J, Griffiths AD, Winter G, Chiswell DJ. Phage antibodies: Filamentous phage displaying antibody variable domains. Nature. 1990;348(6301):552-4. doi:10.1038/348552a0
21. Ledsgaard L, Kilstrup M, Karatt-Vellatt A, McCafferty J, Laustsen AH. Basics of antibody phage display technology. Toxins. 2018;10(6):236. doi:10.3390/ toxins10060236
22. Nelson AL. MAbs. 2010;2(1):77-83. doi:10.4161/ mabs.2.1.10786
23. Weisser NE, Hall JC. Applications of single-chain variable fragment antibodies in therapeutics and diagnostics. Biotechnol Adv. 2009;27(4):502-20. doi:10.1016/j.biotechadv.2009.04.004
24. Jafari B, Hamzeh-Mivehroud M, Moosavi-Movahedi AA, Dastmalchi S. Identification of novel single-domain antibodies against FGF7 using phage display technology. SLAS Discov. 2018;23(2):193-201. doi:10.1177/2472555217728520
25. Alizadeh AA, Hamzeh-Mivehroud M, Farajzadeh M, Moosavi-Movahedi AA, Dastmalchi S. A simple and rapid method for expression and purification of functional TNF-alpha using GST fusion system. Curr Pharm Biotechnol. 2015;16(8):707-15. doi:10.2174/138 92010160815060315254 9
26. Wu S, Zhang Y. Lomets: A local meta-threading-server for protein structure prediction. Nucleic Acids Res. 2007;35(10):3375-82. doi:10.1093/nar/gkm251
27. Gopalakrishnan K, Sowmiya G, Sheik SS, Sekar K. Ramachandran plot on the web (2.0). Protein Pept Lett. 2007;14(7):669-71. doi:10.2174/092986607781483912
28. Modi V, Xu Q, Adhikari S, Dunbrack RL, Jr. Assessment of template-based modeling of protein structure in casp11. Proteins. 2016;84 Suppl 1(Suppl 1):200-20. doi:10.1002/prot.25049
29. Kaczor AA, Bartuzi D, Stępniewski TM, Matosiuk D, Selent J. Protein-protein docking in drug design and discovery. Methods Mol Biol. 2018;1762:285-305. doi:10.1007/978-1-4939-7756-7_15
30. Hamers-Casterman C, Atarhouch T, Muyldermans S, Robinson G, Hamers C, Songa EB, et al. Naturally occurring antibodies devoid of light chains. Nature. 1993;363(6428):446-8. doi:10.1038/363446a0
31. Chiu ML, Goulet DR, Teplyakov A, Gilliland GL. Antibody structure and function: The basis for engineering therapeutics. Antibodies (Basel). 2019;8(4):55. doi:10.3390/antib8040055
32. Vermeer AW, Norde W. The thermal stability of immunoglobulin: Unfolding and aggregation of a multi-domain protein. Biophys J. 2000;78(1):394-404. doi:10.1016/s0006-3495(00)76602-1
33. Nessler I, Khera E, Vance S, Kopp A, Qiu Q, Keating TA, et al. Increased tumor penetration of single-domain antibody-drug conjugates improves in vivo efficacy in prostate cancer models. Cancer Res. 2020;80(6):1268-78. doi:10.1158/0008-5472.can-19-2295
34. Pourtaghi-Anvarian S, Mohammadi S, Hamzeh-Mivehroud M, Alizadeh AA, Dastmalchi S. Characterization of the novel anti-TNF-α single-chain fragment antibodies using experimental and computational approaches. Prep Biochem Biotechnol. 2019;49(1):38-47. doi:10.1080/10826068.2018.1487855
35. Niccheri F, Real-Fernàndez F, Ramazzotti M, Lolli F, Rossi G, Rovero P, et al. Human recombinant domain antibodies against multiple sclerosis antigenic peptide csf114(glc). J Mol Recognit. 2014;27(10):618-26. doi:10.1002/jmr.2386
36. Yang J, Yan R, Roy A, Xu D, Poisson J, Zhang Y. The i-tasser suite: Protein structure and function prediction. Nat Methods 2015;12(1):7-8. doi:10.1038/nmeth.3213
37. Chae YK, Ranganath K, Hammerman PS, Vaklavas C, Mohindra N, Kalyan A, et al. Inhibition of the fibroblast growth factor receptor (fgfr) pathway: The current landscape and barriers to clinical application. Oncotarget 2017;8(9):16052-74. doi:10.18632/ oncotarget.14109
38. Lensen JF, Rops AL, Wijnhoven TJ, Hafmans T, Feitz WF, Oosterwijk E, et al. Localization and functional characterization of glycosaminoglycan domains in the normal human kidney as revealed by phage display-derived single chain antibodies. J Am Soc Nephrol. 2005;16(5):1279-88. doi:10.1681/asn.2004050413
39. Martínez-Torrecuadrada J, Cifuentes G, López-Serra P, Saenz P, Martínez A, Casal JI. Targeting the extracellular domain of fibroblast growth factor receptor 3 with human single-chain fv antibodies inhibits bladder carcinoma cell line proliferation. Clin Cancer Res. 2005;11(17):6280-90. doi:10.1158/1078-0432.ccr-05-0282